One-Pot Synthesis of Multicomponent (Mo, Co) Metal Sulfide/Carbon Nanoboxes as anode materials for Improving Na-ion Storage

Juan Xiang, [a] and Taeseup Song [a]

[a] Department of Energy Engineering, Hanyang University, Seoul 133-791, South Korea.

E-mail: tssong@hanyang.ac.kr

Experimental Section

Material preparation

Preparation of ZIF-67 nanocrystals: ZIF-67 was prepared according to a previously reported process.[1] In a typical synthesis procedure, 1 mmol cobalt nitrate hexahydrate and 4 mmol of 2-methylimidazole were added into 25.0 mL of methanol, respectively. After they were totally dissolved, the latter solution was added into the former under magnetic agitation for 1 min and then stood for 24 h. The purple solid was collected after centrifugation, washed with methanol for several times, and dried at room temperature.

Synthesis of $MoS_2/Co_9S_8/C$: As-prepared ZIF-67 (50 mg) was dispersed into glucose solution (0.025 M) by sonication for 10 min, followed by the addition of Na2MoO4·2H2O (0.6 mmol) and thiourea (4 mmol). After 10-min stirring, the solution was transferred into a 50 mL Teflon-lined stainless steel autoclave and maintained at 200 °C for 24 h. After naturally cooling to room temperature, the black precipitate was collected by centrifugation, washed with ethanol and deionized water for several times, and vacuum-dried at 60 °C overnight. The as-prepared cobalt-molybdenum precursor (donated as CoMo-precursor) sample was further annealed at 500 °C in argon atmosphere for 4 h with a ramping rate of 2 °C min^{-1} to obtain the highly crystalline sample. For comparison, pure Co_9S_8 and MoS_2 samples were synthesized according to a similar route except the addition of Na2MoO4·2H2O and ZIF-67, respectively. To study the contribution of carbon sodium capacity, pure carbon was synthesized according to a similar route with glucose as starting material.

Material Characterization

The samples were characterized by field-emission scanning electron microscope (FESEM; JEOLJSM07600F) and transmission electron microscope (TEM; JEOL JEM-2100F). Element mapping was analyzed by EDX attached to the TEM instrument. The chemical composition and surface valance states were analyzed with an X-ray photoelectron spectrometer (XPS, VG Microtech ESCA2000). XRD patterns of the products were explored by A Rigaku D/MAX RINT-2000 X-Ray Diffractometer (XRD) with Cu Kα radiation at a voltage of 40 kV and a current of 40 mA. Thermogravimetric analysis (TGA) was performed with a ramp rate of 10 °C min^{-1} in air atmosphere.

Electrochemical measurements

The working electrode is made of active materials, conductivity agent (Carbon black), and binder (polyvinylidene fluoride) with a weight ratio of 8:1:1 and 1.0 M $NaCF_3SO_3$ in diethylene glycol dimethyl ether with 5% fluoroethylene carbonate (FEC) additive was used as the electrolyte. The mass loading of the electrode was controlled to between 1.3- 1.8 mg. Sodium metal was used as both the reference electrode and counter electrode. In an argon-filled glove box, the coin-type half cells were assembled and then tested in TOSCAT 3000 battery tester (TOSCAT 3000, Toyo Systems, Tokyo, Japan) within a voltage range from 0.01 to 3.0 V. Cyclic voltammetry measurements were conducted on an Autolab potentiostat/galvanostat (PGSTAT-72637) electrochemical workstation. Electrochemical Impedance Spectroscopy (EIS) for each sample was taken within a frequency range of 1 MHz to 10 mHz and with a voltage amplitude ΔV= 5 mV.

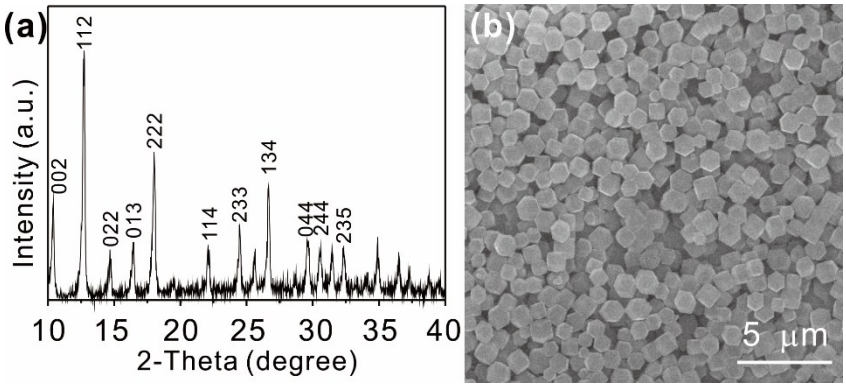

Fig. S1 XRD pattern (a) and FESEM image (b) of ZIF 67 nanocrystals.

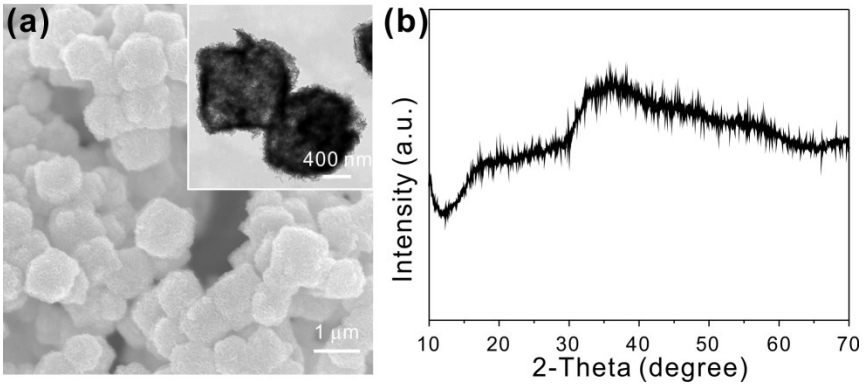

Fig. S2 (a) SEM images of CoMo-precursor, inset in (a) is the TEM image of CoMo-precursor; (b) XRD pattern of CoMo-precursor.

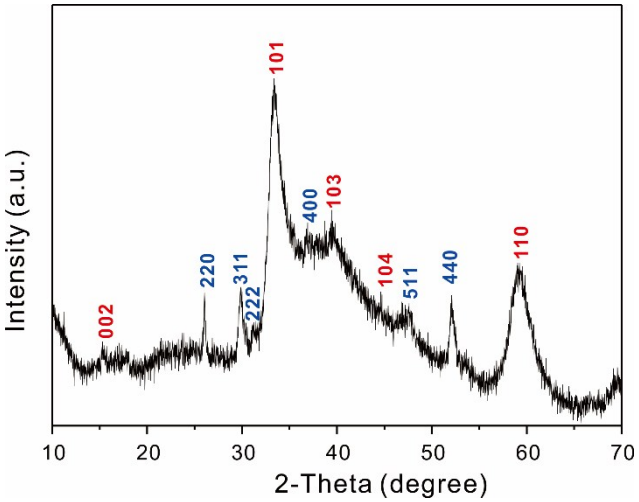

Fig. S3 XRD pattern of $MoS_2/Co_8S_9/C$ nanoboxes.

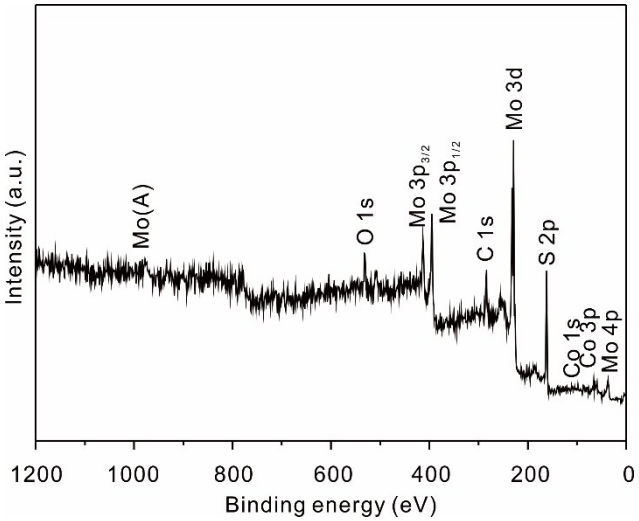

Fig. S4 XPS spectrum of $MoS_2/Co_8S_9/C$ nanoboxes.

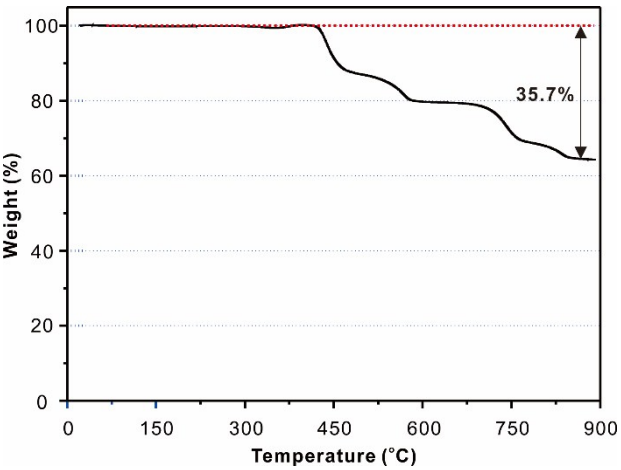

Fig. S5 TG curve of MoS_2/Co_8S_9/C nanoboxes.

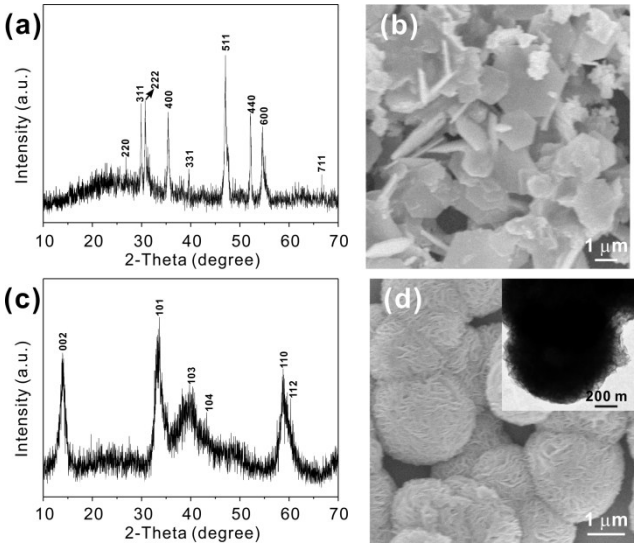

Fig. S6 (a) XRD pattern and (b) SEM image of single-phased Co_9S_8; (c) XRD pattern and (d) SEM image of single-phased MoS_2, inset in (d) is the TEM image of single-phased MoS_2.

.

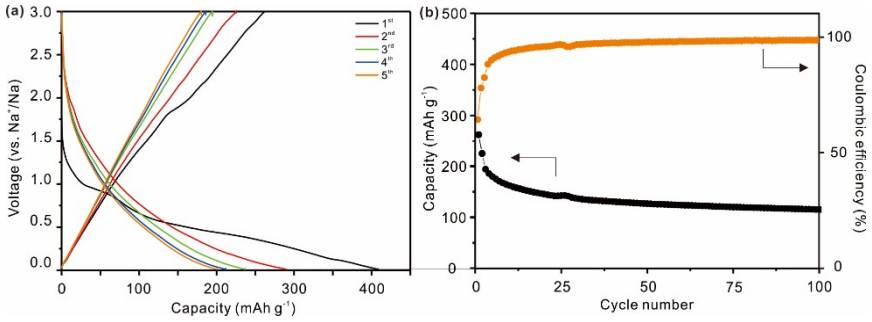

Fig. S7 (a) Typical voltage profile, and (b) Cycling performance of carbon at a current density of 200 mA g^{-1}.

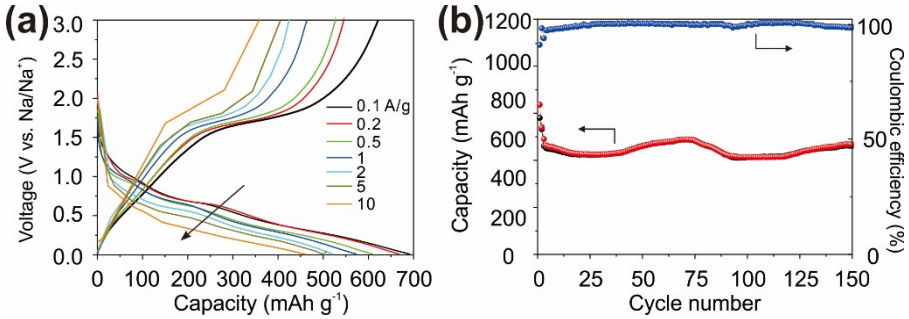

Fig. S8 (a) Typical voltage profile of MoS_2/Co_8S_9/C nanoboxes between 0.01 and 3.0 V at the rate from 0.1 to 10 A g^{-1}; (b) Cycling performance of MoS_2/Co_8S_9/C nanoboxes at a current density of 1 A g^{-1}.

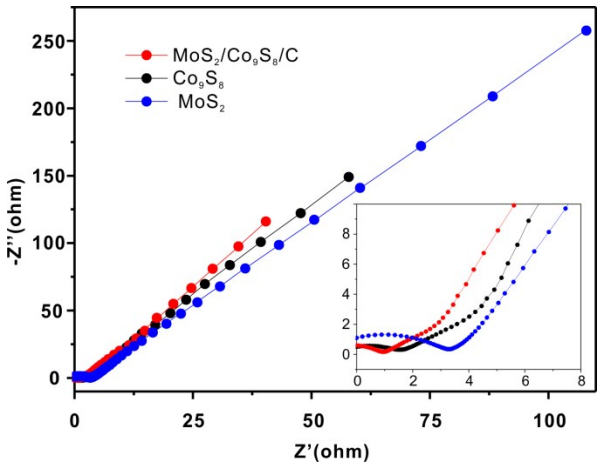

Fig. S9 The Nyquist plots of single-phased Co_9S_8, single-phased MoS_2 and $MoS_2/Co_8S_9/C$ nanoboxes electrode before cycling.

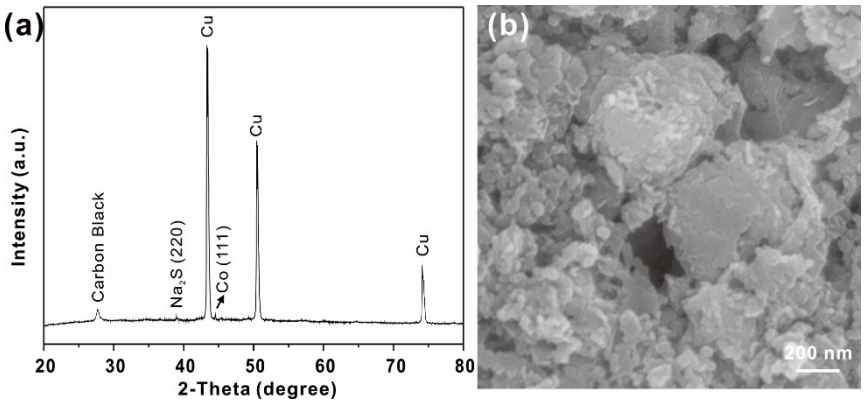

Fig. S10 (a) *Ex situ* XRD patterns of the $MoS_2/Co_9S_8/C$ nanoboxes after 1st discharge and (b) SEM image of the $MoS_2/Co_9S_8/C$ nanoboxes after 100 cycles.

Table S1. Comparison of the electrochemical performance of MoS_2/Co_9S_8/C nanobox with previously reported metal sulfides/mixed metal sulfides anode materials for NaIBs

Materials	**Current density [mA g^{-1}]**	**Cycle**	**Capacity[mAh g^{-1}]**	**Rate capability**	**Reference**
MoS_2/C paper	**80**	**100**	**286.0**	205 mAh g^{-1} at 1000 mA g^{-1}	**[2]**
MoS_2 nanosheets	**40**	**100**	**386**	251 mAh g^{-1} at 320 mA g^{-1}	**[3]**
MoS_2/C tube	**250**	**200**	**480**	370 mAh g^{-1} at 2500 mA g^{-1}	**[4]**
MoS_2/GR spheres	**200 (1500)**	**50 (600)**	**480 (323)**	234 mAh g^{-1} at 10 A g^{-1}	**[5]**
MoS_2/GR	**100 (1000)**	**50 (500)**	**340 (300)**	230 mAh g^{-1} at 5 A g^{-1}	**[6]**
Co_9S_8/C sphere	**500**	**50**	**404**	326 mAh g^{-1} at 1.5 A g^{-1}	**[7]**
Co_9S_8/MWCNT	**500 (2000)**	**80(80)**	**444 (373)**	-	**[8]**
MoS_2/TiO_2 nanowires	**20**	**100**	**191**	48 mAh g^{-1} at 4 A g^{-1}	**[9]**
MoS_2/SnS nanocrystal	**500**	**100**	**455**	238 mAh g^{-1} at 7 A g^{-1}	**[10]**
Ni_3S_2@MoS_2 nanofiber	**200 (5000)**	**100 (400)**	**602 (277)**	283 mAh g^{-1} at 5 A g^{-1}	**[11]**
MoS_2/Co_9S_8 nanobox	**500 (1000)**	**100 (150)**	**546 (461)**	222 mAh g^{-1} at 10 A g^{-1}	**Current work**

References

1. Z. Jiang, W. Lu, Z. Li, K. H. Ho, X. Li, X. Jiao, D. Chen, *J. Mater. Chem. A,* **2014**, *2*, 8603-8606.

2. X. Xie, T. Makaryan, M. Zhao, K. L. Van Aken, Y. Gogotsi, G. Wang, *Adv. Energy Mater.* **2016**, *6*, 1502161.

3. D. Su, S. Dou, G. Wang, *Adv. Energy Mater.* **2015**, *5*, 1401205.

4. X. Zhang, X. Li, J. Liang, Y. Zhu, Y. Qian, *Small* **2016**, *12*, 2484-2491.

5. S. H. Choi, Y. N. Ko, J.-K. Lee, Y. C. Kang, *Adv. Funct. Mater.* **2015**, *25*, 1780-1788.

6. S. Kalluri, K. H. Seng, Z. Guo, A. Du, K. Konstantinov, H. K. Liu, S. X. Dou, *Sci. Rep.* **2015**, *5*, 11989.

7. Y. N. Ko, Y. C. Kang, *Carbon* **2015**, *94*, 85-90.

8. H. Zhou, J. Hu, *Mater. Lett.* **2017**, *195*, 26-30.

9. J.-Y. Liao, B. D. Luna, A. Manthiram, *J. Mater. Chem. A* **2016**, *4*, 801-806.

10. S. H. Choi, Y. C. Kang, *ACS Appl. Mater. Interfaces* **2015**, *7*, 24694-26702.

11. J. Wang, J. Liu, H. Yang, D. Chao, J. Yan, S. V. Savilov, J. Lin, Z. X. Shen, *Nano Energy* **2016**, *20*, 1-10.